Protein oleogels prepared by solvent transfer method with varying protein sources

Annika Feichtinger, Dieke Groot Nibbelink, Suzanne Poppe, Lucas Bozzo, Jasper Landman, Elke Scholten[*]

Physics and Physical Chemistry of Foods, Wageningen University & Research, P.O. Box 17, 6700 AA, Wageningen, The Netherlands

A B S T R A C T

The increasing interest in plant-based materials warrants investigating whether a method used to create protein oleogels by a solvent transfer of whey protein aggregates can be applied to other (specifically plant-based) types of globular proteins. Our results demonstrate that the solvent transfer procedure is indeed suitable to also obtain fully plant-based protein oleogels. Protein aggregates in water – the starting point for the solvent transfer – were shown to be of similar size for all protein sources ($\sim$ 200 nm), which gave the opportunity to further investigate the effect of protein characteristics. The aggregates maintained a well-dispersed state throughout the solvent transfer procedure for whey and potato protein isolate aggregates, whereas large agglomerates (20–50 μm) were formed for egg, pea and soy protein isolate aggregates. At native protein concentration, the smaller aggregate size for whey and potato protein oleogels led to higher gel strengths (protein concentration 7 and 10%, G' $\sim$ 2800 Pa) due to more efficient network formation. Next to aggregate size, the gel strength was also related to the hydrophobicity of protein aggregates, apparent from the difference in gel strength between oleogels of similarly sized whey (G' of 2800 Pa) and potato protein aggregates (G' of 350 Pa) when diluted to the same protein concentration (7%). In an apolar environment, the higher hydrophobicity of potato protein aggregates led to weaker attractive interactions compared to the more hydrophilic whey protein aggregates. These results show that the gel strength of protein oleogels can be controlled by both protein aggregate size and protein characteristics.

1. Introduction

The current transition from animal-based to plant-based ingredients poses many challenges if the original physical properties of a food product should be maintained. In the case of lipids, which are a major ingredient in many food products, the solid character of fats is often crucial to provide the typical, desired product characteristics. Even though different plant-based solid fats are available, in particular the predominantly used palm fat is heavily criticized for the large environmental impact of its production, such as loss of biodiversity and deforestation. From an environmental perspective, these effects could be countered by using a more diverse range of locally grown oils like sunflower oil or rapeseed oil as a source of lipids (Parsons, Raikova, & Chuck, 2020; Schmidt, 2015). Next to the environmental impact, liquid oils are also preferred from a nutritional perspective, as the consumption of *trans*-fatty acids and – though debated – saturated fatty acids has been

associated with negative effects on health (de Souza et al., 2015; Li et al., 2015; Mensink & Katan, 1990; Mozaffarian, Katan, Ascherio, Stampfer, & Willett, 2006; Phillips et al., 2012). In search of alternatives to circumvent these undesired aspects of solid fats surrounding sustainability and health, attempts have been made to structure liquid oils to obtain oleogels with solid-like properties. One of the more recent structurants that has been used for this purpose are proteins, as they have a high nutritional value, are affordable and widely accepted by consumers.

In the last years, several approaches to prepare oleogels with protein as a structurant have been developed (Feichtinger & Scholten, 2020), of which the most commonly applied one is the emulsion-templated approach (Abdolmaleki, Alizadeh, Nayebzadeh, Hosseini, & Shahin, 2020; Alizadeh, Abdolmaleki, Nayebzadeh, & Hosseini, 2020; Patel et al., 2015; Qiu, Huang, Li, Ma, & Wang, 2018; Romoscanu & Mezzenga, 2006; Tavernier, Patel, Van der Meeren, & Dewettinck, 2017;

Wijaya, Van der Meeren, Wijaya, & Patel, 2017, 2019), followed by the foam-templated approach (Abdollahi, Goli, & Soltanizadeh, 2020; Ali-zadeh et al., 2020; Chen & Zhang, 2020; Mohanan, Tang, Nickerson, & Ghosh, 2020). Here, a protein-based oil-in-water emulsion or a foam is prepared first, and then dried to remove the water. In case of foams, the dried material is subsequently immersed in oil, which is absorbed by the dried structure and thereby immobilized. These methods have been applied using several types of (plant) proteins. However, in both the emulsion- and foam-templated approach, polysaccharides are often added in addition to protein, to obtain emulsions or foams that are stable enough to endure the drying process. As the preparation process depends on an optimal stability of the emulsions or foams, these methods are also rather sensitive toward changes in the applied protein concentration and the protein-to-polysaccharide ratio. Furthermore, the material obtained in templated approaches is technically only an oleogel after it has been sheared, because only then the continuous protein-polysaccharide-network becomes the dispersed phase, while the oil becomes the continuous one. Alternatively, proteins can also be used directly as the dispersed phase using a solvent-transfer method. In this procedure, heat-set protein aggregates are transferred from water to oil via an intermediate solvent, and the process is rather robust regarding variations in the preparation process (de Vries, Wesseling, van der Linden, & Scholten, 2017). As the protein aggregates are present as the dispersed phase in the form of a space-spanning protein network, the oleogel properties can be further adjusted after obtaining the initial oleogel by adjusting the protein volume fraction, or by adjusting the strength of the interactions between the protein aggregates. This is possible for example by adding small amounts of water or heating to increase capillary interactions or van der Waals interactions, respectively (de Vries, Jansen, van der Linden, & Scholten, 2018).

The described solvent transfer method for the preparation of protein oleogels has so far only been applied to whey protein isolate (WPI) (de Vries, Wesseling, et al., 2017). It is not known if this method can also be used to create oleogels with other types of globular proteins. Moreover, it is not yet understood which protein characteristics determine the properties of the obtained oleogels and how these characteristics influence the protein network formation. Due to the increasing demand of plant-based products, it is of specific interest to study different types of plant proteins as a structurant. Generally, the functionality of plant-based proteins, like solubility, gelling or foaming ability, is often considered inferior compared to animal-based proteins. Therefore, a direct substitution of animal proteins by plant proteins is usually challenging. These differences in functionality are due to structural differences between plant- and animal proteins, which arise from their distinct native environment. For example, milk and egg proteins are found in aqueous environments and accordingly are mostly hydrophilic. In contrast, plant proteins are typically storage proteins. They generally have larger and more compact structures, are more hydrophobic and as a consequence also less soluble (Day, Cakebread, & Loveday, 2022; Kim, Wang, & Selomulya, 2020). Typical examples for storage proteins are soy and pea protein, which form oligomeric structures (Kim et al., 2020). The solubility and protein characteristics are also affected by the extraction process, as the sometimes harsh conditions can lead to denaturation and aggregation of the proteins (Day et al., 2022).

The aim of this paper is to investigate whether the solvent transfer procedure can be applied to other globular proteins than whey protein, and how the differences in protein characteristics influence the network formation and final properties of the resulting protein oleogels. Next to three different plant proteins, potato (PoPI), pea (PPI) and soy (SPI) protein isolate, we also include egg protein isolate (EPI) as a second animal-based protein in addition to whey protein isolate (WPI), which was used as a reference. The oleogels were compared regarding their oil holding capacity, size of the protein aggregates in water and oil, network structure and rheological properties.

2. Materials and methods

2.1. Materials

For the preparation of the protein oleogels, five protein isolates of different origin were used: Whey protein isolate (WPI) (BiPRO 9500, Agropur, Le Sueur, MN, U.S.), egg protein isolate (EPI) (egg protein isolate 90, Bouwhuis Enthoven, Raalte, The Netherlands), potato protein isolate (PoPI) (Solanic 200, Avebe, Veendam, The Netherlands), pea protein isolate (PPI) (Emsland pea protein Empro E86, Emlichheim, Germany) and soy protein isolate (SPI) (SUPRO 500E IP, Solae LLC, St. Louis, MO, U.S.). Reddy sunflower oil (Vandemoortele Nederland BV, Zeewolde, The Netherlands) was purchased at a local supermarket. The fluorescent dyes Prodan (*N,N*-Dimethyl-6-propionyl-2-naphthylamine) and Rhodamine B were obtained from Sigma-Aldrich (St. Louis, MO, U. S.). Acetone (AR-grade) and ethanol (96 %vol) were obtained from Actu-All chemicals (Oss, The Netherlands) and VWR chemicals (Amsterdam, The Netherlands), respectively. For all experiments, demineralized water was used.

2.2. Methods

2.2.1. Preparation of protein oleogels

Protein oleogels were prepared based on a solvent transfer method as described previously (de Vries, Wesseling, et al., 2017), with slight adjustments for the different protein types.

2.2.1.1. Preparation of protein isolate solutions. Aqueous protein solutions were prepared by adding the protein isolates to demineralized water and stirring for 2 h at room temperature. Concentrations of protein isolate solutions were 5 wt% for WPI and SPI, 4 wt% for EPI and PoPI, and 8 wt% for PPI, which were chosen individually per protein source to obtain small aggregates of comparable size during a later heating step. The solutions were stored in the fridge overnight, to ensure complete hydration of the proteins. SPI, PoPI and WPI dissolved well. However, as EPI and PPI did not dissolve sufficiently well, further steps were added to this procedure: For EPI, after 2 h of stirring, the solution was homogenized with a rotor-stator-homogenizer (T25 digital Ultra Turrax, IKA-Werke, Staufen, Germany), left overnight, and then again homogenized. Then the solution was centrifuged at 4600 g for 15 min (at 20 °C) to remove insoluble material. For PPI, the pH of the protein isolate solution was adjusted to 8 after the first hour of stirring. After the second hour of stirring, the pH was measured again and re-adjusted if necessary. The PPI-solutions were homogenized with a rotor-stator-homogenizer, left overnight, and homogenized again the next day. Then, they were further homogenized with a 2-stage homogenizer (LabhoScope Homogenizer, Delta instruments, Sofia, Bulgaria) for four rounds at 200 bar. After centrifugation at 2000g for 15 min (at 20 °C), the pellet was discarded and the supernatant was collected as the final PPI-solution.

2.2.1.2. Preparation of protein aggregates in water and solvent transfer to oil. To obtain protein aggregates of comparable size, pH, heating time and temperature were adjusted individually per protein source for the different protein isolate solutions. For WPI-solutions, the pH was adjusted to approximately 5.95, for PoPI to 4.2, for EPI to 6.5, for PPI to 6.8 and for SPI to 5.6. The solutions were heated in 50 mL plastic tubes with screwcaps in a water bath; for WPI-, EPI- and SPI-solutions for 15 min at 85 °C, for PoPI-solutions for 30 min at 90 °C and for PPI-solutions for 30 min at 92 °C. The resulting protein aggregate dispersions were cooled on ice for 5 min, and then homogenized with a rotor-stator homogenizer (T25 digital Ultra Turrax, IKA-Werke, Staufen, Germany) to deagglomerate the obtained sub-micron protein aggregates. For WPI, SPI and PoPI, the homogenized suspensions were centrifuged at 4000 g for 20 min (20 °C) to collect the pellet, which was then redispersed

(using a rotor-stator-homogenizer) and centrifuged two more times in demineralized water (ratio of protein pellet:water of approximately 1:10 by volume). These washing steps were subsequently repeated two or three times with acetone, and two times with oil. For EPI- and PPI-aggregate dispersions, it was necessary to adjust the pH to 6 to be able to harvest the aggregates by centrifugation; for these two protein isolates, the two washing steps with water were omitted. Instead, the solvent transfer procedure was carried out immediately by applying two or three washing steps in acetone, followed by two washing steps in sunflower oil. For all washing steps, pellets were redispersed in a ratio of approximately 1:10 using a rotor-stator-homogenizer, and the protein dispersion was centrifuged at 4000 g for 20 min (20 °C). After the last centrifugation step of the protein-in-oil-dispersions, the obtained pellets were anew dispersed in a ratio of approximately 1:10 in sunflower oil, and left in the fume hood overnight under gentle stirring for remaining acetone to evaporate. The next day, gel formation was induced by a final centrifugation step at 4000 g for 20 min (20 °C). All oleogels were prepared in duplicate. Before use for further experiments, they were mixed using a rotor-stator homogenizer in order to ensure homogeneity.

2.2.2. Particle size distributions of aqueous gels and oleogels

Particle size distributions (PSDs) of the different protein aggregates in water as well as of protein aggregates in oil as obtained after the solvent transfer were measured by static light scattering with a Malvern Mastersizer 2000, either with a Hydro 2000SM dispersion unit for aqueous samples, or a manual dispersion unit AWM2002 for oleogels (Malvern Instruments Ltd, Worcestershire, UK). Results were obtained based on the Mie theory as a mathematical model; the refractive index for water was set to 1.33, to 1.47 for sunflower oil, and to 1.45 and 1.54 for protein aggregates in water and in oil, respectively. Samples were prepared by diluting the aqueous pellet or oleogel in a ratio of approximately 1:10 with water or sunflower oil, respectively, and homogenizing with a rotor-stator homogenizer (T25 digital Ultra Turrax, IKA-Werke, Staufen, Germany). Additionally, the PSDs of these diluted aggregate suspensions were also determined after sonication (BRANSON Ultrasonics Corporation, Danbury, CT, U.S.). To prevent overheating of the samples, they were sonicated in pulse mode (0.5 s on, 0.5 s off) with an amplitude of 50% for 5 min. PSD-measurements were done in triplicate for two separately prepared oleogels per protein source and the averaged volume-based distributions are reported, from which the volume weighted mean diameters $d_{4,3}$ were obtained.

2.2.3. Protein content of oleogels and oil holding capacity

The protein content of oleogels was determined by Dumas. Before combustion in a Flash EA 1112 N/protein analyzer (Thermo Scientific, Waltham, MA, U.S.), samples were dried in an oven at 60 °C overnight. The conversion factors to calculate the protein concentration from the determined nitrogen concentrations (protein content = N x conversion factor) were 6.38, 5.74, 6.25, 5.45 and 5.71 for WPI, EPI, PoPI, PPI and SPI, respectively. Measurements were done in triplicate for WPI, and in quadruplicate for all other protein sources, for two separately prepared oleogels per protein source.

The oil holding capacity of the obtained oleogels, i.e. the amount of oil a material can absorb, was obtained based on a common centrifugation method (Wang, Maximiuk, Fenn, Nickerson, & Hou, 2020). In short, after the last centrifugation step performed at 4000 g for 20 min, the protein concentration of the pellets was determined. The oil holding capacity was taken as the inverse of the protein content of these final oleogels.

2.2.4. Water content of oleogels

The water content of oleogels was determined by dry matter content determination. Approximately 1 g of sample was placed on pre-heated aluminum cups in an oven (Venticell, BMT Medical Technology, Brno, Czech Republic) at 105 °C for approximately 4 h. To calculate the water content, the weight of the samples before and after drying was recorded

in duplicate, for two separately prepared oleogels for each protein type.

2.2.5. Hydrophobicity of protein aggregates

The hydrophobicity of the different protein aggregates was determined by a Prodan assay. A 0.064 mM solution of the fluorescent dye Prodan (*N,N*-Dimethyl-6-propionyl-2-naphthylamine) in acetone was prepared freshly on the day of use. Protein aggregates of the different protein isolates in water were prepared as described in section 2.2.1. To ensure that the protein aggregates were deagglomerated, the suspensions obtained after heating were first homogenized with a rotor-stator homogenizer (T25 digital Ultra Turrax, IKA-Werke, Staufen, Germany), and then sonicated, as described in section 2.2.2. The protein content of these dispersions was determined by Dumas as described in section 2.2.3, and the dispersions were then diluted to obtain 6 samples with a protein concentration ranging from 0 to 0.01 wt%. As a standard, an unheated WPI-solution was used, to be able to correct results for daily fluctuations in the procedure. Prodan-solution and diluted protein aggregate dispersions were added to acrylic cuvettes (type 67.755, 10 × 10 × 45 mm, Sarstedt AG & Co., Nümbrecht, Germany) in a ratio by volume of 1:400, and mixed by vortexing. For sample blanks, acetone instead of Prodan-solution was added to the protein aggregate dispersions. After storage for 15 min in the dark at room temperature, the relative fluorescence intensity (RFI) of samples was measured with a fluorimeter (Luminescence Spectrometer LS-50B, PerkinElmer, Waltham, MA, U.S.) at an excitation wavelength of 365 nm and emission wavelength of 440 nm. Each sample was measured in duplicate. The net RFI-values were calculated by subtracting the respective blank values from the values measured for protein aggregate suspensions, and the hydrophobicity was obtained as a dimensionless value as the slope of net RFI-values versus protein concentration. Relative hydrophobicity of the samples was expressed as a number on a scale from 0 to 1, setting the highest obtained value for the slope as 1.

2.2.6. Confocal laser scanning microscopy (CLSM)

To gain insights into the protein network structure before and after the solvent transfer, for all different protein types, CLSM-images were taken of aqueous pellets as obtained after the first centrifugation step in water and of the final oleogels. Protein aggregates in aqueous pellets were stained with a 0.2 wt% Rhodamine B solution in water, and oleogels with a 0.2 wt% Rhodamine B solution in ethanol. Aqueous pellets and oleogels were diluted fivefold with water or sunflower oil, respectively, homogenized with a rotor-stator-homogenizer (T25 digital Ultra Turrax, IKA-Werke, Staufen, Germany), and then the respective dye solution was added in a ratio of dye solution:aggregate dispersion of 1:1000. After addition of the dye, the samples were mixed by vortexing, and stored overnight in the fridge protected from light. Then the samples were again centrifuged at 4000 g for 20 min to obtain the stained pellet, which was examined under a LSM 510 - ConfoCor 2 confocal laser scanning microscope (Zeiss, Oberkochen, Germany) after careful mixing with a spatula. To verify that the addition of dye did not lead to changes in the network structure, PSDs and rheological properties were measured for the stained samples and compared to the results of unstained samples. In order to make all components in the images visible, images were partly nonlinearly adjusted (gamma adjustment) with the software ImageJ.

2.2.7. Oscillatory rheology

To quantify macroscopic gel properties of the oleogels prepared from different protein types, oscillatory rheology was performed. First, the protein concentration of the oleogels was adjusted to five different concentrations in case of WPI- and PoPI-oleogels, or four in case of EPI-, PPI- and SPI-oleogels (WPI 3–7%, PoPI 4–10%, EPI and PPI 10–13%, SPI 5–9%). This was done by addition of sunflower oil to the oleogels as obtained after the last centrifugation step (see 2.2.1) and thorough mixing by manual stirring with a spatula. Then the samples were degassed with a vacuum pump for approximately 5 min to remove air

bubbles. Measurements were performed with a shear-controlled MCR 502 rheometer with a parallel plate system (Anton Paar GmbH, Graz, Austria). To prevent the occurrence of slip, sand-blasted plates were chosen (upper plate model PP50/S, lower plate Inset I-PP50/SS/S, diameter 50 mm). After a pre-shear period of 30 min at an amplitude of 0.01% and a frequency of 1 Hz for the samples to equilibrate, the frequency was kept constant at 1 Hz, and the amplitude was increased from 0.01 to 1000% within 520 s. The frequency of 1 Hz was within the linear viscoelastic regime for all samples, as was confirmed by preceding frequency sweep tests, in which the frequency was increased from 0.01 to 100 Hz within 600 s at a constant amplitude of 0.01%. Frequency sweeps were performed on the oleogel samples of lowest protein concentration, where the highest frequency dependence is typically observed (over a range of 0.01–7.6 Hz, values of the exponent n for $G' \sim \omega^n$ were ≤ 0.1 for all different oleogel types). From the amplitude sweeps, the point of the G' (storage modulus)-curves at which G' had decreased by 5% from its initial value was determined using the instrument software. The strain value at this point was defined as the limit of linearity, γ_0, and the corresponding G'-value as plateau value of G'. Measurements were done in duplicate on two separately prepared oleogel samples. An overview of the protein concentrations at which rheological tests for the different oleogel types were performed and the results for the frequency sweeps can be found in Table S1 and Figure S2 in the supplementary information.

2.2.8. Determination of fractal dimensions

Protein gels often show self-similar structures at different length scales, and the network structure can be quantified by the determination of a fractal dimension D_f based on rheological measurements (Andoyo, Dianti Lestari, Mardawati, & Nurhadi, 2018). The rheological parameters G' (storage modulus) and γ_0 (limit of linearity) are related to the volume fraction, φ, in a power-law fashion as:

$$G' = \varphi^A \qquad (1)$$

$$\gamma_0 = \varphi^B \qquad (2)$$

By linearization, the exponents A and B are obtained as the slope of the log-log plot between the rheological parameters and the volume fraction φ (Andoyo et al., 2018). In our study, we assume the volume fraction φ to be proportional to the protein concentration. Based on the relation between the limit of linearity γ_0 and volume fraction φ, gel networks can be classified into two types according to the model of Shih, Shih, Kim, Liu, and Aksay (1990); the strong-link and weak-link regime. In the strong-link regime, γ_0 decreases with increasing protein concentration, and interactions between fractal flocs are stronger than within flocs. In the weak-link regime, γ_0 increases with increasing protein concentration, and interactions between flocs are weaker than within flocs. In this model, only two extreme situations are considered: the macroscopic elasticity of the gel, G', is either only determined by the elasticity of the links within flocs (strong-link, at low particle concentrations) or only by the elasticity of links between flocs (weak-link, at high particle concentrations) (Shih et al., 1990). To account for an intermediate situation, this model has been extended by Wu & Morbidelli (2001), to consider a third possible situation, in which inter- and intrafloc interactions both deliver a relevant contribution to the elasticity of the gel network, described by the transition regime. Table 1

provides an overview of the definition of the factors A and B and the classification of the different regimes for both models.

2.2.9. Statistical analysis

To confirm that differences in rheological properties (gel strength, limit of linearity) of different oleogel types were statistically significant, a single factor variance analysis (ANOVA) was performed, followed by a Tukey's HSD test to compare mean values at a significance level of $p = 0.05$.

3. Results and discussion

3.1. Oleogel preparation and composition

The starting point to prepare protein oleogels based on the solvent transfer method are heat-set protein aggregates dispersed in water. To be able to investigate how protein characteristics influence the network formation and final properties of the oleogels, we aimed to start the solvent transfer procedure with protein aggregates of a comparable size. By adjusting the pH-value, protein concentration and heating conditions for each protein isolate solution, we were able to obtain sub-micron protein aggregates of a size of approximately 200 nm for all different protein sources (Fig. 1a).

As the initial building blocks had a similar size, differences in network formation and properties of the oleogels thus arouse from other differences in the protein (aggregate) characteristics. The effect of varying protein characteristics for the different protein sources already became clear during the solvent transfer. For PoPI- and SPI-aggregates, the same procedure as for WPI-aggregates could be applied, as the protein aggregates could be easily harvested by centrifugation. However, for the EPI- and PPI-aggregates, centrifugation did not yield a significant amount of pellet of the protein aggregates. This may be due to the fact that these aggregates were less agglomerated, or had a lower density. To counter this effect, the pH of the protein aggregate dispersions was reduced to 6 to induce further agglomeration, which allowed to harvest the protein aggregate pellet. In acetone, aggregates of all protein sources investigated could be harvested by centrifugation without difficulties, which is likely related to the larger density difference between protein aggregates and acetone. In addition, dehydration of the protein aggregates in an increasingly apolar environment probably increased the density of the protein aggregates. For EPI- and PPI-aggregates, any still dissolved protein and salts contained in the protein isolates were removed during these washing steps with acetone, and therefore also here only protein aggregates were present after the final washing step in oil, even though the washing steps in water were omitted.

After centrifugation of the final oil dispersion, we obtained a gel-like pellet for all protein types with a protein content ranging between 8 and 13%. The low amounts of water ($\leq 1.3\%$) left in the oleogels after the solvent transfer procedure show that water could be efficiently removed for all different protein types (Table 2). The small amount of remaining water in the oleogels is assumed to be firmly absorbed within the protein aggregates, and is therefore not removed during the solvent transfer. These results demonstrate that it is indeed possible to obtain protein oleogels with different animal- as well as plant-based globular proteins

Table 1

Overview of different possible regimes and definitions of factors A and B according to the scaling models of Shih et al. (1990) and Wu and Morbidelli (2001).

Fractal model	Regime		A	B
Shih et al.	strong-link		$(3 + x)/(3 - D_f)$	$-1(1 + x)/(3 - D_f)$
	weak-link		$1/(3 - D_f)$	$1/(3 - D_f)$
Wu and Morbidelli	strong-link	$\alpha = 0$	$\beta/(3 - D_f)$	$(3 - \beta - 1)/(3 - D_f)$
	weak-link	$\alpha = 1$	with $\beta = 1 + (2 + x)(1 - \alpha)$	
	transition	$0 < \alpha < 1$		
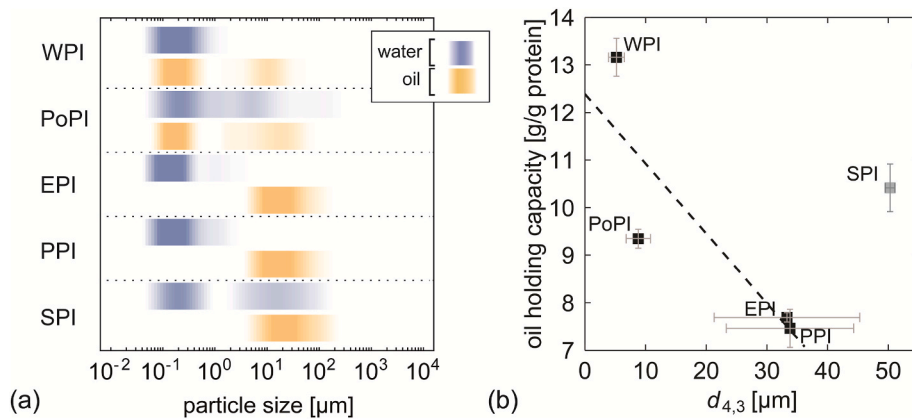
Fig. 1. (a) PSDs of protein aggregates in water and oil prepared from protein isolates of different origins. Volume frequencies are indicated by color intensity. To deagglomerate aggregates, aqueous samples were treated by sonication, and oil suspensions by homogenization. (b) Oil holding capacity (OHC) of the different oleogel types as a function of average particle size ($d_{4,3}$). The dashed line is added to guide the eye and indicates the trend observed for the black data points. (For interpretation of the references to color in this figure legend, the reader is referred to the Web version of this article.)

Table 2

Composition of protein oleogels from varying protein sources (pellet obtained after final centrifugation of protein aggregate dispersions in oil, 4000 g) and oil holding capacity (OHC = 100/prot. conc.).

|	WPI	PoPI	EPI	PPI	SPI
Protein concentration of pellet after final centrifugation step (%)	7.6 ± 0.4	10.7 ± 0.2	13.0 ± 0.1	13.4 ± 0.4	9.6 ± 0.5
Water content (%)	0.8 ± 0.3	0.2 ± 0.1	1.2 ± 0.4	1.3 ± 0.2	0.5 ± 0.1
Oil holding capacity (g/g protein)	13.2	9.3	7.7	7.5	10.5

by applying the solvent transfer method.

As described in the methods section, the oil holding capacity (OHC) of these final oil pellets was calculated as the inverse of the protein content (Table 2). The differences in the OHC were related to the differences in aggregate size of the protein aggregates in oil as obtained after the solvent transfer: As shown in Fig. 1a, for WPI- and PoPI- aggregates, the protein building blocks of a size of approximately 200 nm formed in water were found back in the oleogels, which was not the case for protein aggregates from EPI, PPI and SPI. Instead, for these protein aggregates a main peak in the PSDs between 10 and 100 μm was obtained. This indicates that for these proteins, the initially small aggregates extensively agglomerated during the solvent transfer process. For the oleogels, deagglomeration prior to determination of the PSDs was performed with a rotor-stator-homogenizer instead of by sonication as for the aqueous suspensions, as in case of the oleogels additional sonication did not lead to further deagglomeration (see supplementary information, Figure S1). Fig. 1b shows the OHC as a function of the protein aggregate size in oil. Besides for SPI-oleogels (grey symbol), a trend of a decreasing OHC with increasing aggregate size was observed (black symbols), as indicated with the dashed line. Compared to small aggregates, large aggregates are less efficient in forming a network due to a lower surface area. Therefore, centrifugation leads to denser oleogel pellets with less incorporated oil in case of larger aggregates, i.e. a higher protein concentration and a lower OHC. Only for SPI-oleogels, the OHC was still relatively high, even though the aggregate size in oil was the highest. This may be explained by different effects: SPI-aggregates could have a higher porosity, and therefore a larger oil absorption capacity (Zayas, 1997). Possible mechanisms for the observed changes of the protein aggregate size throughout the solvent transfer procedure as well as differences in the structure of protein aggregates and the formed networks in water and oil will be discussed further in the following section based on CLSM-images.

3.2. Structural changes of aggregates and their networks during solvent transfer by CLSM

The difference in protein network formation in oil as observed based on the PSDs (Fig. 1a) was also confirmed by CLSM-imaging (Fig. 2). In the case of WPI and PoPI, a homogenous network structure in oil based on small protein aggregates is observed. Even though for PoPI-oleogels some larger agglomerates are visible, they are composed of only loosely agglomerated, smaller particles. This is consistent with the smaller particle sizes measured in oil for these two protein types. However, in the case of EPI-, PPI- and SPI-oleogels, the CLSM-images show the presence of large, dense particles or agglomerates disrupting the network structure, which is as well in agreement with the particle size measurements. The large agglomerates appear less dense and somewhat porous for SPI-oleogel. This increased porosity compared to EPI- and PPI-agglomerates in oil could explain the comparably high OHC of SPI-oleogel despite the large aggregate size.

From the CLSM-images (Fig. 2), more information regarding the change of the network structure when transferring the aggregates from water to oil can be obtained. Network formation is determined by the interactions between the protein aggregates. Due to heat-induced denaturation, the unfolding of the globular proteins exposes their hydrophobic groups. In water, the increased hydrophobicity of the formed protein aggregates results in an attractive interaction between the aggregates (Israelachvili, 2011). Whereas WPI-aggregates were found to have the lowest hydrophobicity (0.435), all other protein aggregates had a significantly higher hydrophobicity, with the highest value obtained for PoPI-aggregates (0.964) (Fig. 2). Based on the hydrophobicity of the protein aggregates, in water we would therefore expect the lowest attractive interactions between WPI-aggregates, as these aggregates were most hydrophilic. This can indeed be observed by the more homogeneous distribution of the WPI-aggregates. As the hydrophobicity of the other proteins was much higher, we expect more network formation, which is indeed also observed.

In oil, the situation is the opposite: hydrophobic interactions are of repulsive nature and increase the solvation of protein aggregates in the oil phase, whereas hydrophilic patches of the protein aggregates provide attractive interactions (de Vries, Gomez, van der Linden, & Scholten, 2017). The observed densification of the network structures in oil for all protein types indicates that the attractive forces resulting from hydrophilic interactions in oil are stronger than the hydrophobic interactions in water for all protein types. This also becomes apparent when comparing the gel strength of oleogels with the respective aqueous gels, which was exemplarily done for WPI- and SPI-gels. The aqueous gels had a significantly lower gel strength compared to the oleogels (see supplementary information, Figure S3). Similar observations were made by de Vries, Hendriks, van der Linden, and Scholten (2015) on hydrogel-templated WPI-oleogels. Compression tests showed that the
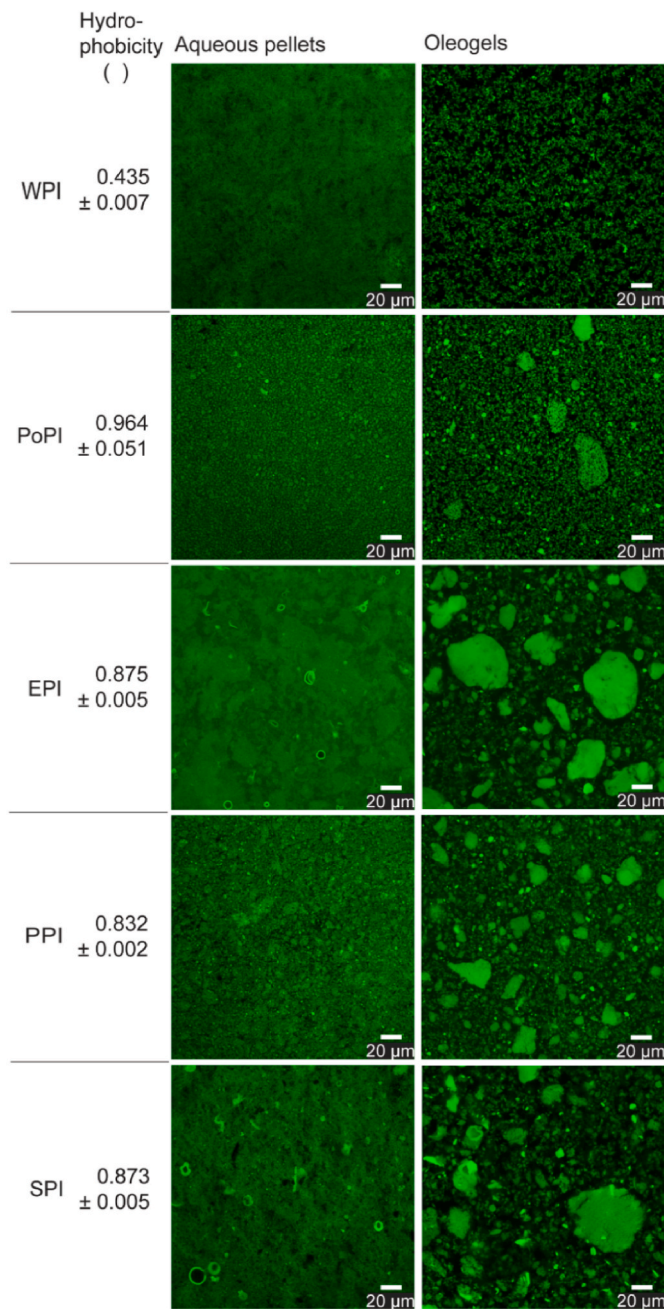
Fig. 2. CLSM-images of aqueous gels and oleogels as obtained after centrifugation of the aggregate suspensions in water or oil at 4000 g. Images of EPI aqueous gels and oleogels and images of PPI- and SPI-oleogels were nonlinearly adjusted (gamma adjustment), in order to make both smaller and larger aggregates visible. The values determined for hydrophobicity of the protein aggregates in water are provided for each protein source.

oleogels were significantly stronger than the corresponding hydrogels due to stronger attractive interactions between proteins in oil than in water.

In addition to the general densification of the network structure upon transfer to the oil phase, we found that the effect of the solvent transfer was different for protein aggregates from different sources, as apparent in the preservation of homogeneously dispersed aggregates for WPI and PoPI, and the formation of larger, dense agglomerates in case of EPI, PPI and SPI. Even though these large agglomerates were not yet present in the aqueous environment, for these protein types the interactions between the protein aggregates became significant enough to induce

extensive agglomeration when changing the polarity of the solvent. As hydrophilic interactions are assumed to be of main importance for the net attraction between protein aggregates in oil (de Vries, Gomez, et al., 2017), their hydrophobicity is an important factor to take into account in order to explain these observed differences.

Intuitively, one could expect that more hydrophobic aggregates would agglomerate less in oil. However, our results suggest the opposite. According to the CLSM-images, the WPI-aggregates with the lowest hydrophobicity agglomerated the least, and showed a more homogenous network structure of evenly dispersed fine particles, whereas the more hydrophobic EPI-, PPI- and SPI-aggregates showed the most agglomeration and the networks appear more heterogenous with less well dispersed aggregates (Fig. 2). These results indicate that the network structure is not only determined by the interactions in oil, but also by changes in the interactions during the solvent transfer procedure, and the initial state of the aggregates in water. Possibly, the fact that the transfer of WPI-aggregates started from a situation in which the aggregates were well-dispersed ensured that the aggregates were maintained in a well-dispersed state during the solvent transfer, despite the increase of attractive interactions. EPI-, PPI- and SPI-aggregates were already slightly agglomerated in the water phase, due to the stronger hydrophobic interactions, and the protein aggregates were already in close proximity before initiation of the solvent transfer procedure. Upon transfer to oil, the increasingly strong attractive forces with an increasing relevance of hydrophilic interactions led to further agglomeration, and prevented better dispersibility in oil, despite their higher hydrophobicity. In case of PoPI-aggregates, the formation of large, dense agglomerates may have been prevented due to their comparatively favorable particle-solvent interactions. PoPI-aggregates had the highest hydrophobicity amongst the several protein types, and therefore the smallest increase in attractive interactions between the aggregates in the course of the solvent transfer. In addition, the PoPI-aggregates in water appeared to be dispersed more evenly compared to EPI-, PPI- and SPI-aggregates, which could be another reason preventing the formation of large agglomerates upon the solvent transfer.

As the network formation may not be explained by differences in hydrophobicity only, it is likely that other factors related to differences in protein characteristics also contribute to differences in the behavior of the various aggregate types during the solvent transfer. One aspect that could be related to the formation of large agglomerates is the formation of covalent disulfide bonds. From the amount of cysteine groups occurring in the different proteins as found in literature (Gorissen et al., 2018), we expect sulfhydryl groups to mainly occur in whey and egg proteins. However, as this would lead to more aggregate formation for these proteins, this effect does not match our results. Another aspect that could influence the dispersibility of the different protein aggregates in the different solvents could be the density or porosity of the aggregates, which may have varied for the different protein types. To confirm this assumption, the density of the protein aggregates would need to be determined in oil as a continuous phase. Although we have tried several approaches, we were not able yet to identify a reliable method.

As clear from the presented results, we do not find general differences in the behavior of animal- and plant-based protein aggregates. Instead, the differences in behavior seem to originate from specific properties of the protein aggregates, which do not necessarily and directly depend on if the protein is animal- or plant-based.

These results show that network formation in oil can be obtained for different protein types, but that the network structure depends greatly on the type of protein. Even when the initial protein building blocks are of similar size, differences in protein characteristics and changes in the interactions during the solvent transfer process lead to differences in network formation.
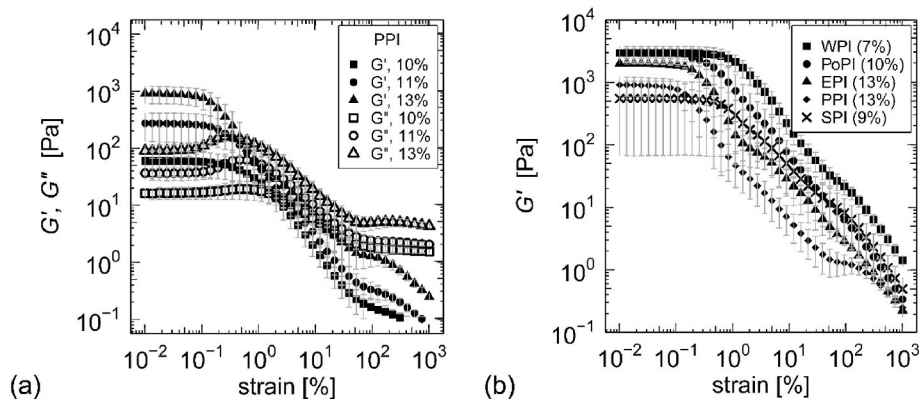
Fig. 3. (a) Storage modulus G' (closed symbols) and loss modulus G'' (open symbols) as a function of strain for PPI-oleogels at different protein concentrations. (b) G' as a function of strain for oleogels prepared from different protein sources at maximum protein concentration.

3.3. Rheological properties

3.3.1. Gel strength and limit of linearity

To gain more insights into the gel properties of the oleogels, oscillatory rheology was performed. Exemplary results of the amplitude sweeps of PPI-oleogels at three different protein concentrations are shown in Fig. 3a. For all other oleogels, the obtained curve progressions where similar. At low strain, the storage modulus G' is larger than the loss modulus G'', and both moduli have a constant value. When a specific strain is reached, a crossover of the moduli takes place, after which $G'' > G'$, i.e. viscous properties dominate as the gel structure breaks down. For G'', a small increase of the strain can be observed before the gel network breaks, i.e. before the crossover of G' and G'' takes place. This behavior, where an overshoot is observed in G'', but not in G', can be classified as a weak strain overshoot, and is related to first structural rearrangements in the network before it finally breaks. The explanation for the observed behavior of a weak strain overshoot depends on the specific microstructure of the sample at hand (Hyun et al., 2011). In our case, the temporary increase in G'' could be explained by the increasing shear rate first leading to increased contact and interactions between separate flocs in the network, and thereby the formation of new clusters and a higher flow resistance, before a final breakdown of the floc backbone occurs, leading to a decrease of both G' and G'' (Hyun et al., 2011; Xia, Siu, & Sagis, 2021). As visible from the examples shown for PPI-oleogels in Fig. 3a, the effect of a strain overshoot in G'' is more pronounced for oleogels with a higher gel strength, i.e. a higher protein concentration. This is explained by an increasing particle volume fraction and thereby increasing number of contact points in the system with an increasing protein content, which leads to a more pronounced effect of microscopic structural rearrangements.

Whereas the rheological responses for the different oleogel types were comparable, the G'-values in the linear regime as well as the length of the linear regime γ_0 varied (Fig. 3b). The G'-values in the linear region were determined to characterize the gel strength. Fig. 3b shows the results for the different oleogels at the maximum protein concentration as obtained after centrifugation. The highest gel strength was obtained for WPI-oleogels, even though the protein concentration was the lowest (7%). The second strongest oleogel was PoPI- (10%), followed by EPI- (13%), PPI- (13%) and SPI- (9%) oleogels. One explanation for the differences in gel strength are the differences in aggregate size. Fig. 4 shows the relation between G'-values obtained for the different oleogels and aggregate size. For the oleogels at maximum protein concentration (square symbols), a clear trend to a decreasing gel strength with increasing aggregate size is visible, as indicated with the dashed line. As discussed earlier, the effect of aggregate size is related to an increased surface area and thereby increased amount of interactions and a more efficient network formation at smaller particle sizes, which was also
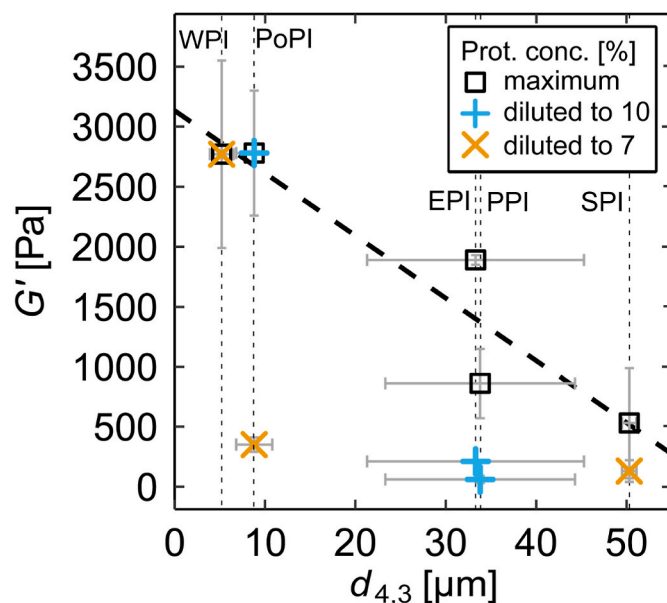
Fig. 4. Storage modulus G' of different oleogel types at maximum protein concentration (WPI = 7%, PoPI = 10%, EPI = 13%, PPI = 13%, SPI = 9%), as well as diluted to lower protein concentrations (10%, plus symbols, or 7%, cross symbols), as a function of average particle size ($d_{4,3}$). Dashed lines were added to guide the eye.

reflected in the oil holding capacity (Fig. 1b). In our case, WPI- and PoPI-oleogels had the smallest aggregates in oil, as was shown by PSD-measurements and CLSM-images, and therefore also had the highest gel strength. This explains why these gels have a higher gel strength even though the protein content was low. The aggregate size thus seems to be an important factor not only for the oil holding capacity, but also the gel strength.

However, when comparing the gel strength of different oleogels at the same protein concentration, it becomes apparent that the aggregate size cannot be the only factor determining the gel strength. Fig. 4 shows, where available, next to the G'-values obtained at maximum protein concentration (square symbols) also the G'-values of oleogels diluted to a protein concentration of 10% (plus symbols) or 7% (cross symbols). When comparing the gel strength at equal protein concentrations (10% or 7%), PoPI-oleogels still had a slightly higher gel strength (2800 Pa at 10%, 350 Pa at 7%) than EPI- (210 Pa at 10%), PPI- (60 Pa at 10%) and SPI-oleogels (130 Pa at 7%), but a significantly lower gel strength than WPI-oleogels (2800 Pa at 7%). As aggregates in WPI- and PoPI-oleogels were of comparable size, this is most likely related to differences in the

strength of interactions between the protein aggregates. Attractive interactions are expected to be higher in case of WPI-oleogels, due to the lower hydrophobicity of the WPI-aggregates compared to PoPI-aggregates (Fig. 2), and therefore a larger degree of attractive hydrophilic interactions is present in the WPI-oleogels at the same protein concentration. From this, we conclude that the most important parameters which determine the gel strength of oleogels is the size as well as the hydrophobicity of the protein aggregates.

Next to differences in the gel strength, differences in the limit of linearity (γ_0) are also apparent (Fig. 3b). The value of γ_0 can be understood as an indication of the brittleness of the oleogels, with a higher limit of linearity indicating a lower brittleness. WPI-oleogels with the lowest protein concentration had the highest value for γ_0. This may be explained by the fact that these oleogels had the smallest aggregates, and therefore the largest number of connection points, which makes the network more resistant towards deformation. PoPI-oleogel with similarly small aggregates had a lower value for γ_0, which shows that also the strength of the interactions plays an important role. The weaker interactions between PoPI-aggregates provide less resistance to deformation. As the aggregate size increased for EPI- and PPI-oleogels, the values for γ_0 decrease.

However, as apparent from Fig. 3b, SPI-oleogels had a high value for γ_0, even though the particle size was large. This sample also had a high value for the OHC, which we attribute to the possible porous nature of these large agglomerates as seen by CLSM-images. In case the large SPI-agglomerates indeed also incorporate oil within themselves, the network present in the SPI-oleogels could be seen as a continuous network, with regions of lower and regions of higher density (the larger agglomerates). The comparably strong interactions in the high-density regions may keep these regions stable against deformation up to higher strain rates, which would explain the relatively high limit of linearity. For both the results of the gel strength and limit of linearity as shown in Figs. 4 and 3b, respectively, the results of the statistical analysis regarding the significance of the discussed differences can be found in the supplementary information (Table S2).

3.3.2. Fractal dimensions

Next to the CLSM-images, information regarding the network structure of the oleogels can also be obtained by a characterization of the protein networks in terms of scaling theories based on rheological data as obtained from amplitude sweeps. The model of Shih et al. (1990) has been previously applied to characterize protein networks, for example WPI- (Alting, Hamer, de Kruif, & Visschers, 2003; Andoyo, Guyomarc'h, Burel, & Famelart, 2015; Hongsprabhas, Barbut, & Marangoni, 1999; Kuhn, Cavallieri, & da Cunha, 2010; Marangoni, 2000; Vreeker, Hoekstra, den Boer, & Agterof, 1992), EPI- (Ould Eleya, Ko, & Gunasekaran, 2004), SPI- (Bi, Li, Wang, & Adhikari, 2013) and PPI- (Yang, Zamani,

Liang, & Chen, 2021) networks in water, as well as WPI-networks in oil (de Vries, Wesseling, et al., 2017). These theories are only valid for systems that show self-similarity over different length scales. However, as visible from CLSM-images (Fig. 2), our oleogels show a heterogenous structure with partly large differences in aggregate size, and therefore may not be self-similar on a sufficiently large length scale to apply such a fractal model (Nicolai, 2007). Especially in the case of EPI-, PPI- and SPI-oleogels, large aggregates were present which clearly disrupted the network. Although these oleogels may not be considered to be real fractal structures, these theories can still provide valuable information on differences in the network structure.

Fig. 5 shows the limit of linearity γ_0 and the storage modulus G', obtained from amplitude sweeps, as a function of the protein concentration. From the slope of these curves (factor A and B in equations (1) and (2)), the fractal dimensions D_f were calculated, according to the model of Shih et al. (1990) and the model of Wu and Morbidelli (2001) (for different models, see Table 1). As the results obtained based on the model of Shih et al. (1990) were not realistic, we show here only the results calculated based on the model of Wu and Morbidelli (2001) (Table 3). For the results obtained based on the model of Shih et al. (1990), see Table S3 in the supplementary information. That this model was not suitable to describe our samples is obvious from the values obtained for the fractal dimension of the backbone x. The value of x should be in a range of $1 \leq x < D_f$ (Shih et al., 1990), whereas we find values for $x < 1$, and even partially negative values (Table S3). This could be explained by the fact that, as mentioned previously, the model of Wu and Morbidelli (2001) also takes into account an intermediate regime, whereas the model of Shih et al. (1990) considers only the two unlikely, extreme situations of either only inter- or only intra-link contributions. According to the model of Wu and Morbidelli (2001), our oleogels are indeed clearly in the transition regime, as α-values were found to be between 0.3 and 0.6 (Table 3), which indicates that both inter- and intra-links had a relevant contribution to our systems.

Table 3
Fractal dimensions D_f and value of factor α as determined based on rheology data according to the fractal model of Wu and Morbidelli (2001). Values for α were calculated for a value of the fractal dimension of the backbone x of 1 and 1.3. For results according to the model of Shih et al. (1990), see Table S3 in the supplementary information.

	x	WPI	PoPI	EPI	PPI	SPI
D_f		2.47 ± 0.07	2.43 ± 0.06	2.67 ± 0.01	2.71 ± 0.01	2.47 ± 0.05
α	1	0.48 ± 0.08	0.30 ± 0.11	0.44 ± 0.03	0.40 ± 0.03	0.45 ± 0.04
	1.3	0.58 ± 0.08	0.40 ± 0.11	0.54 ± 0.03	0.50 ± 0.03	0.55 ± 0.04
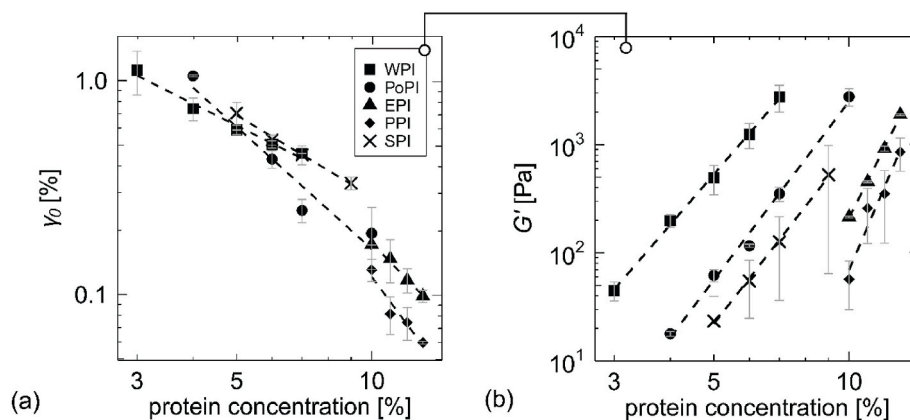
Fig. 5. (a) Limit of linearity γ_0 and (b) storage modulus G' as a function of protein concentration for oleogels prepared from different protein sources. Dashed lines are added to guide the eye.

With the model of Wu and Morbidelli (2001), lower values for the fractal dimension D_f were obtained for WPI-, PoPI- and SPI-oleogels (D_f = 2.4–2.5) compared to those obtained for EPI- and PPI-oleogels (D_f = 2.7). A D_f-value closer to 3 indicates more compact structures, whereas a value closer to 2 means that the flocs have a more loose or diffuse structure (Vreeker et al., 1992). Based on the CLSM-images, we expected low D_f-values for WPI- and PoPI-oleogels as they provided more open and homogenous networks, and higher values for the other oleogels as they showed more agglomeration and thus a denser network. We indeed found low D_f-values for WPI- and PoPI-oleogels, but also for SPI-oleogels (Table 3). Although the result for SPI do not reflect the network structure, they do coincide with the results for the OHC, as we found a higher OHC for WPI-, PoPI- and SPI-oleogels. The higher D_f-values for the EPI- and PPI-oleogels coincide with the lower values for the OHC. Therefore, while the oleogel networks may not be considered fractal, the calculated fractal dimensions seem to be a good indication of the density of the networks.

To the best of our knowledge, there is no literature available regarding the determination of fractal dimensions of protein oleogels, besides the D_f-value previously calculated for WPI-oleogels by de Vries, Wesseling, et al. (2017), which had been prepared with the same approach. In that work, a fractal dimension of 2.2 was calculated based on the model of Shih et al. (1990) , similar to what was found in this work when using the model of Shih et al. (1990), see Table S3. Apart from the results of de Vries, Wesseling, et al. (2017), the only D_f-values available for comparison in literature are for aqueous protein gels. In previous researches on gels prepared with different protein types a wide range of D_f-values was found (1.6–2.8) (Alting et al., 2003; Andoyo et al., 2015; Bi et al., 2013; Hongsprabhas et al., 1999; Kuhn et al., 2010; Marangoni, 2000; Ould Eleya et al., 2004; Vreeker et al., 1992; Yang et al., 2021). This wide range of D_f-values is explained by differences in gelation mechanisms and environmental conditions, as well as the influence of protein extraction methods on protein characteristics (Yang et al., 2021). These factors probably have a greater influence on the aggregation behavior than the choice of the protein source itself. It is therefore difficult to directly compare our D_f-values with values obtained for aqueous gels in literature. Moreover, our results were likely influenced by the high heterogeneity of the network structures. Nevertheless, our results do show that different types of proteins are able to provide networks of varying structures in oil, and had fractal dimensions in a range as expected based on aqueous protein gels.

4. Conclusions

Our experiments show that heat-set protein aggregates of different globular animal- and plant-based sources can be used to structure liquid oils, using a solvent transfer method. The method opens the door towards the design of fully plant-based, vegan oleogels. For efficient network formation to occur in the oil phase, it was found crucial to obtain homogenously dispersed protein aggregates in oil, as opposed to the formation of large agglomerates. Our results suggest that this depends both on differences in the protein characteristics as well as on the degree of agglomeration of the protein aggregates in water – i.e. before the solvent transfer. From more evenly dispersed protein aggregates in water, as was the case for WPI- and PoPI-aggregates, oleogels with small particle size were obtained. The gel strength of the different oleogels was found to mainly depend on two factors. First, with increasing aggregate size in oil, the gel strength decreased due to a decrease in surface area and therefore less possibilities for network formation. Secondly, the hydrophobicity of protein aggregates was found to influence the gel strength. A higher hydrophilicity leads to stronger attractive hydrophilic interactions in an oil phase. As WPI-aggregates were smallest and had the highest hydrophilicity, WPI-oleogels were strongest of all protein sources tested. For PoPI-oleogels, which had a comparable aggregate size but higher hydrophobicity than WPI-oleogels, the weaker interactions were noticeable in a lower limit of linearity compared to WPI-

oleogels. The gel strength of PoPI-oleogels, however, was comparable at slightly higher protein concentrations. Therefore, we conclude that as long as protein aggregates can be prevented from agglomeration during the solvent transfer, we are able to create plant-based protein oleogels with comparable properties as for animal-based proteins in similarly efficient ways.

CRediT authorship contribution statement

Annika Feichtinger: Conceptualization, Methodology, Investigation, Writing – original draft, Visualization. **Dieke Groot Nibbelink:** Investigation, Writing – review & editing. **Suzanne Poppe:** Investigation, Writing – review & editing. **Lucas Bozzo:** Methodology, Writing – review & editing. **Jasper Landman:** Conceptualization, Methodology, Writing – review & editing, Visualization, Supervision. **Elke Scholten:** Conceptualization, Writing – review & editing, Supervision, Project administration, Funding acquisition.

Declaration of competing interest

The authors declare that they have no known competing financial interests or personal relationships that could have appeared to influence the work reported in this paper.

Appendix A. Supplementary data

Supplementary data to this article can be found online at https://doi.org/10.1016/j.foodhyd.2022.107821.

References

Abdollahi, M., Goli, S. A. H., & Soltanizadeh, N. (2020). Physicochemical properties of foam-templated oleogel based on gelatin and xanthan gum. *European Journal of Lipid Science and Technology, 122*(2), Article 1900196. https://doi.org/10.1002/ejlt.201900196

Abdolmaleki, K., Alizadeh, L., Nayebzadeh, K., Hosseini, S. M., & Shahin, R. (2020). Oleogel production based on binary and ternary mixtures of sodium caseinate, xanthan gum, and guar gum: Optimization of hydrocolloids concentration and drying method. *Journal of Texture Studies, 51*(2), 290–299. https://doi.org/10.1111/jtxs.12469

Alizadeh, L., Abdolmaleki, K., Nayebzadeh, K., & Hosseini, S. M. (2020). Oleogel fabrication based on sodium caseinate, hydroxypropyl methylcellulose, and beeswax: Effect of concentration, oleogelation method, and their optimization. *Journal of the American Oil Chemists' Society, 97*(5), 485–496. https://doi.org/10.1002/aocs.12341

Alting, A. C., Hamer, R. J., de Kruif, C. G., & Visschers, R. W. (2003). Cold-set globular protein gels: Interactions, structure and rheology as a function of protein concentration. *Journal of Agricultural and Food Chemistry, 51*(10), 3150–3156. https://doi.org/10.1021/jf0209342

Andoyo, R., Dianti Lestari, V., Mardawati, E., & Nurhadi, B. (2018). Fractal dimension analysis of texture formation of whey protein-based foods. *International Journal of Food Science*, 1–17. https://doi.org/10.1155/2018/7673259, 2018.

Andoyo, R., Guyomarc'h, F., Burel, A., & Famelart, M.-H. (2015). Spatial arrangement of casein micelles and whey protein aggregate in acid gels: Insight on mechanisms. *Food Hydrocolloids, 51*, 118–128. https://doi.org/10.1016/j.foodhyd.2015.04.031

Bi, C. H., Li, D., Wang, L. J., & Adhikari, B. (2013). Viscoelastic properties and fractal analysis of acid-induced SPI gels at different ionic strength. *Carbohydrate Polymers, 92*(1), 98–105. https://doi.org/10.1016/j.carbpol.2012.08.081

Chen, K., & Zhang, H. (2020). Fabrication of oleogels via a facile method by oil absorption in the aerogel templates of protein–polysaccharide conjugates. *ACS Applied Materials & Interfaces.* https://pubs.acs.org/doi/abs/10.1021/acsami.9b21435.

Day, L., Cakebread, J. A., & Loveday, S. M. (2022). Food proteins from animals and plants: Differences in the nutritional and functional properties. December 2021 *Trends in Food Science & Technology, 119*, 428–442. https://doi.org/10.1016/j.tifs.2021.12.020.

Feichtinger, A., & Scholten, E. (2020). Preparation of protein oleogels: Effect on structure and functionality. *Foods, 9*(12), 1745. https://doi.org/10.3390/foods9121745

Gorissen, S. H. M., Crombag, J. J. R., Senden, J. M. G., Waterval, W. A. H., Bierau, J., Verdijk, L. B., et al. (2018). Protein content and amino acid composition of commercially available plant-based protein isolates. *Amino Acids, 50*(12), 1685–1695. https://doi.org/10.1007/s00726-018-2640-5

Hongsprabhas, P., Barbut, S., & Marangoni, A. G. (1999). The structure of cold-set whey protein isolate gels prepared with Ca++. *Lebensmittel-Wissenschaft und -Technologie-Food Science and Technology, 32*(4), 196–202. https://doi.org/10.1006/fstl.1998.0522

Hyun, K., Wilhelm, M., Klein, C. O., Cho, K. S., Nam, J. G., Ahn, K. H., et al. (2011). A review of nonlinear oscillatory shear tests: Analysis and application of large amplitude oscillatory shear (Laos). *Progress in Polymer Science, 36*(12), 1697–1753. https://doi.org/10.1016/j.progpolymsci.2011.02.002

Israelachvili, J. N. (2011). *Intermolecular and surface forces.* Elsevier. https://doi.org/10.1016/C2009-0-21560-1

Kim, W., Wang, Y., & Selomulya, C. (2020). Dairy and plant proteins as natural food emulsifiers. September *Trends in Food Science & Technology, 105*, 261–272. https://doi.org/10.1016/j.tifs.2020.09.012

Kuhn, K. R., Cavallieri, Â. L. F., & da Cunha, R. L. (2010). Cold-set whey protein gels induced by calcium or sodium salt addition. *International Journal of Food Science and Technology, 45*(2), 348–357. https://doi.org/10.1111/j.1365-2621.2009.02145.x

Li, Y., Hruby, A., Bernstein, A. M., Ley, S. H., Wang, D. D., Chiuve, S. E., et al. (2015). Saturated fats compared with unsaturated fats and sources of carbohydrates in relation to risk of coronary heart disease A prospective cohort study. *Journal of the American College of Cardiology, 66*(14), 1538–1548. https://doi.org/10.1016/j.jacc.2015.07.055

Marangoni, A. (2000). On the structure of particulate gels—the case of salt-induced cold gelation of heat-denatured whey protein isolate. *Food Hydrocolloids, 14*(1), 61–74. https://doi.org/10.1016/S0268-005X(99)00046-6

Mensink, R. P., & Katan, M. B. (1990). Effect of dietary trans fatty acids on high-density and low-density lipoprotein cholesterol levels in healthy subjects. *New England Journal of Medicine, 323*(7), 439–445. https://doi.org/10.1056/NEJM199008163230703

Mohanan, A., Tang, Y. R., Nickerson, M. T., & Ghosh, S. (2020). Oleogelation using pulse protein-stabilized foams and their potential as a baking ingredient. *RSC Advances.* https://pubs.rsc.org/en/content/articlehtml/2020/ra/c9ra07614j.

Mozaffarian, D., Katan, M. B., Ascherio, A., Stampfer, M. J., & Willett, W. C. (2006). Trans fatty acids and cardiovascular disease. *Obstetrical and Gynecological Survey, 61*(8), 525–526. https://doi.org/10.1097/01.ogx.0000228706.09374.e7

Nicolai, T. (2007). Chapter 3. Structure of self-assembled globular proteins. In *Food colloids* (pp. 35–56). Royal Society of Chemistry. https://doi.org/10.1039/9781847557698-00035.

Ould Eleya, M. M., Ko, S., & Gunasekaran, S. (2004). Scaling and fractal analysis of viscoelastic properties of heat-induced protein gels. *Food Hydrocolloids, 18*(2), 315–323. https://doi.org/10.1016/S0268-005X(03)00087-0

Parsons, S., Raikova, S., & Chuck, C. J. (2020). The viability and desirability of replacing palm oil. *Nature Sustainability, 3*(6), 412–418. https://doi.org/10.1038/s41893-020-0487-8

Patel, A. R., Rajarethinem, P. S., Cludts, N., Lewille, B., De Vos, W. H., Lesaffer, A., et al. (2015). Biopolymer-based structuring of liquid oil into soft solids and oleogels using water-continuous emulsions as templates. *Langmuir, 31*(7), 2065–2073. https://doi.org/10.1021/la502829u

Phillips, C. M., Kesse-Guyot, E., McManus, R., Hercberg, S., Lairon, D., Planells, R., et al. (2012). High dietary saturated fat intake accentuates obesity risk associated with the fat mass and obesity–associated gene in adults. *Journal of Nutrition, 142*(5), 824–831. https://doi.org/10.3945/jn.111.153460

Qiu, C., Huang, Y., Li, A., Ma, D., & Wang, Y. (2018). Fabrication and characterization of oleogel stabilized by gelatin-polyphenol-polysaccharides nanocomplexes. *Journal of Agricultural and Food Chemistry, 66*(50), 13243–13252. https://doi.org/10.1021/acs.jafc.8b02039

Romoscanu, A. I., & Mezzenga, R. (2006). Emulsion-templated fully reversible protein-in-oil gels. *Langmuir, 22*(18), 7812–7818. https://doi.org/10.1021/la060878p

Schmidt, J. H. (2015). Life cycle assessment of five vegetable oils. *Journal of Cleaner Production, 87*(C), 130–138. https://doi.org/10.1016/j.jclepro.2014.10.011

Shih, W.-H., Shih, W. Y., Kim, S., Liu, J., & Aksay, I. A. (1990). Scaling behavior of the elastic properties of colloidal gels. *Physical Review A, 42*(8), 4772–4779. https://doi.org/10.1103/PhysRevA.42.4772

de Souza, R. J., Mente, A., Maroleanu, A., Cozma, A. I., Ha, V., Kishibe, T., et al. (2015). Intake of saturated and trans unsaturated fatty acids and risk of all cause mortality, cardiovascular disease, and type 2 diabetes: Systematic review and meta-analysis of observational studies. *BMJ, 351*, h3978. https://doi.org/10.1136/bmj.h3978

Tavernier, I., Patel, A. R., Van der Meeren, P., & Dewettinck, K. (2017). Emulsion-templated liquid oil structuring with soy protein and soy protein: κ-Carrageenan complexes. *Food Hydrocolloids, 65*, 107–120. https://doi.org/10.1016/j.foodhyd.2016.11.008

Vreeker, R., Hoekstra, L. L., den Boer, D. C., & Agterof, W. G. M. (1992). Fractal aggregation of whey proteins. *Topics in Catalysis, 6*(5), 423–435. https://doi.org/10.1016/S0268-005X(09)80028-3

de Vries, A., Gomez, Y. L., van der Linden, E., & Scholten, E. (2017). The effect of oil type on network formation by protein aggregates into oleogels. *RSC Advances, 7*(19), 11803–11812. https://doi.org/10.1039/C7RA00396J

de Vries, A., Hendriks, J., van der Linden, E., & Scholten, E. (2015). Protein oleogels from protein hydrogels via a stepwise solvent exchange route. *Langmuir, 31*(51), 13850–13859. https://doi.org/10.1021/acs.langmuir.5b03993

de Vries, A., Jansen, D., van der Linden, E., & Scholten, E. (2018). Tuning the rheological properties of protein-based oleogels by water addition and heat treatment. *Food Hydrocolloids, 79*, 100–109. https://doi.org/10.1016/j.foodhyd.2017.11.043

de Vries, A., Wesseling, A., van der Linden, E., & Scholten, E. (2017). Protein oleogels from heat-set whey protein aggregates. *Journal of Colloid and Interface Science, 486*, 75–83. https://doi.org/10.1016/j.jcis.2016.09.043

Wang, N., Maximiuk, L., Fenn, D., Nickerson, M. T., & Hou, A. (2020). Development of a method for determining oil absorption capacity in pulse flours and protein materials. *Cereal Chemistry, 97*(6), 1111–1117. https://doi.org/10.1002/cche.10339

Wijaya, W., Sun, Q.-Q., Vermeir, L., Dewettinck, K., Patel, A. R., & Van der Meeren, P. (2019). pH and protein to polysaccharide ratio control the structural properties and viscoelastic network of HIPE-templated biopolymeric oleogels. *Food Structure, 21*, Article 100112. https://doi.org/10.1016/j.foostr.2019.100112

Wijaya, W., Van der Meeren, P., Wijaya, C. H., & Patel, A. R. (2017). High internal phase emulsions stabilized solely by whey protein isolate-low methoxyl pectin complexes: Effect of pH and polymer concentration. *Food & Function, 8*(2), 584–594. https://doi.org/10.1039/c6fo01027j

Wu, H., & Morbidelli, M. (2001). A Model Relating Structure of Colloidal Gels to Their Elastic Properties. *Langmuir, 17*(4), 1030–1036. https://doi.org/10.1021/la001121f.

Xia, W., Siu, W. K., & Sagis, L. M. C. (2021). Linear and non-linear rheology of heat-set soy protein gels : Effects of selective proteolysis of β-conglycinin and glycinin. January *Food Hydrocolloids, 120*, Article 106962. https://doi.org/10.1016/j.foodhyd.2021.106962.

Yang, J., Zamani, S., Liang, L., & Chen, L. (2021). Extraction methods significantly impact pea protein composition, structure and gelling properties. January *Food Hydrocolloids, 117*, Article 106678. https://doi.org/10.1016/j.foodhyd.2021.106678.

Zayas, J. F. (1997). Oil and fat binding properties of proteins. In *Functionality of proteins in food* (pp. 228–259). Springer Berlin Heidelberg. https://doi.org/10.1007/978-3-642-59116-7_5.